Prediction of Grand Minima

Ludwik Liszka and Rickard Lundin

INSTITUTET FÖR RYMDFYSIK
Swedish Institute of Space Physics

Umeå, Sweden

Prediction of Grand Minima

Ludwik Liszka and Rickard Lundin

Swedish Institute of Space Physics
Umeå, Sweden

Prediction of Grand Minima

Ludwik Liszka and Rickard Lundin
Swedish Institute of Space Physics
Umeå, Sweden

Abstract
The aim of this study is to test whether it is possible to predict a Grand Minimum, assuming that there is, in the solar activity, precursor information about the approaching minimum. The monthly averages of sunspot numbers, covering the period from the year 1610 until the present, are used as input data. The time series is converted into a multivariate time series of indicators (the Multiple Indicator Model technique). The multivariate time series for periods including the Maunder and Dalton Minima is used to train a Neural Network model, which is later applied to recent solar sunspot data. The result shows a clear similarity between the periods before the Maunder and Dalton Minima and the period after the year 2000.

Introduction
Grand Minima in solar activity have occurred randomly in historical time. Since these periods of extremely low solar activity seem to have an important impact on the Earth's climate, it would be interesting if a method to predict this phenomenon could be found. In this study monthly values of the solar group sunspot number are used as the input of information. The reason for this is that the above index has been scaled since 1610, and thus represents the longest time series directly describing the solar activity. Unfortunately, after December 1994, the group sunspot number is no longer scaled. After this date the time series is continued using monthly values of sunspot numbers. The input time series is shown in Fig. 1. Since there is no apparent prior information about the approaching Grand Minimum, the input time series has to be processed. An important processing tool is the wavelet transform and its applications: the ampligram and the time scale spectrum.
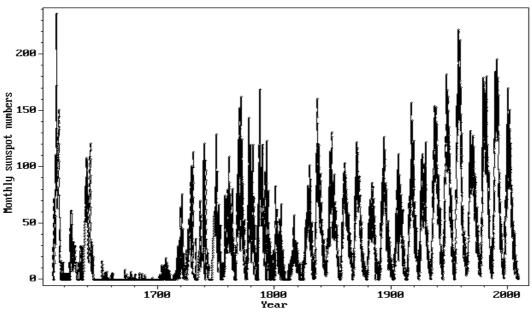

Fig. 1. Monthly sunspot numbers 1610-2009.

1. Wavelet transform

The wavelet transform has become a powerful tool for frequency analysis, in particular for non-stationary time series. Discussions of the wavelet transform and its applications can be found in a number of recent books and review articles (Chui, 1992, Chui et al., 1994, Farge, 1992).

The wavelet transform of a function y(t) is defined as (here * denotes complex conjugation):

$$w(a,b) = a^{-1/2} \int_{-\infty}^{+\infty} y(t)\, g^*((t-b)/a)\, dt \qquad (2)$$

where variable a is the scale dilation parameter and b the translation parameter. Both parameters are dimensionless. The real- or complex-valued function g(t) is called a mother (or analyzing) wavelet.

Here a particular wavelet transform, the Morlet wavelet, will be used. The Morlet wavelet, being a locally periodic wavetrain, is related to windowed Fourier analysis. It is obtained by taking a complex sine wave and localizing it with a Gaussian (bell-shaped) envelope.

The Morlet wavelet is defined as:
$$g(t) = \exp(i\omega_o t - t^2/2) \qquad (3)$$
and its Fourier transform:
$$G(\omega) = \sqrt{2\pi}\, \exp[-(\omega - \omega_o)^2/2] \qquad (4)$$

The Morlet wavelet gives the smallest time-bandwidth product (Lagoutte et al. 1992).
ω_o is a phase constant (in the present study $\omega_o = 5$). For large ω_o the frequency resolution improves, though at the expense of decreased time resolution.

The dilation parameter may be considered as equivalent to the frequency of the analyzed signal, while the translation parameter corresponds to the time elapsed along the analyzed sample. In the present study dilation #1 corresponds to the highest frequency (a half of sampling rate). The highest dilation # corresponds to the lowest observable frequency.

2. Time-series decomposition using wavelet transform

Many time series observed in physics consist of a deterministic part with a superimposed stochastic component. A powerful technique to separate both components has been proposed by Farge (1993) and implemented in practically usable software by Wernik (1997). In that method, being a kind of non-linear filtering (also called the threshold filtering), a wavelet frequency spectrum of the time series is calculated. The time series is decomposed into two parts in the following way:
 - A deterministic "strong" part is obtained by setting to zero all wavelet coefficients less than a certain threshold level. The inverse wavelet transform is used to calculate the corresponding time series.
 - A stochastic "weak" part is obtained by setting to zero all wavelet coefficients greater than that threshold level. The inverse wavelet transform is also used here to calculate the corresponding time series.
- New wavelet spectra are calculated for each partial time series.
Signal discrimination using the magnitude of wavelet coefficients as a discrimination criterion would correspond to discrimination with respect to the spectral density when using the Fourier transform.

The stochastic part must follow a Gaussian probability distribution function. As a measure of departure from a Gaussian distribution the kurtosis is used. If the threshold is properly selected, the integral of the kurtosis of the stochastic part over the entire frequency range reaches a minimum.

3. The ampligram

There is a straightforward generalisation of the above technique (Liszka and Holmström, 1999), which may be used to separate independent components of the signal, assuming that the different components are characterized by different wavelet coefficient magnitudes (spectral densities).

Experience from studies of oscillations in complex mechanical systems indicates that a given oscillation mode usually occurs with a certain amplitude/spectral density. The amplitude ratios between possible modes are usually constant in such a system. That observation may be used to generalize the above non-linear filtering technique. For a time series of N values (N must be an integer power of 2) the following operations are performed:

1. A Morlet wavelet transform is performed with at least 128 dilations. Thus, three N x 128 matrices, A, R and I, are obtained. The matrix A is a matrix of magnitudes of w_{ij}:

$$A = \{|w_{ij}|\} \qquad i=1, \ldots N \qquad j=1, \ldots 128 \qquad (5)$$

R and I contain respective real and imaginary parts of w_{ij}.

2. Instead of using the low-pass or high-pass filtering of wavelet coefficient magnitudes, as described in §2, a kind of band-pass filtering of wavelet coefficient magnitudes is used. The entire range of coefficient magnitudes: 0 to w_{max}, or its lowest 20%, is divided into M intervals such that the k-th interval is limited by:

$$w_{max} * (k-1)/M \quad \text{and} \quad w_{max} * k/M \quad \text{where} \quad k= 1, \ldots M \qquad (6)$$

Two sets of intervals are used in the present work: 10 equal intervals between 0 and 100% of $w_{max \ and}$ in the other set 20 equal intervals between 0 and 20% of w_{max}. For each k the coefficients outside the range defined by (6) are identified and zeroed in matrices R and I, creating two new matrices R_k and I_k. The inverse wavelet transform is performed using R_k and I_k and a new version of the original time series, $y_k(t_i)$, is created. $y_k(t_i)$ is what the signal would look like if only a narrow range of wavelet coefficient amplitude was be present in the signal.

3. The operation is repeated M times at 1 or 10% intervals over the interesting range of coefficient magnitudes, usually 0 - 20% of the maximum wavelet coefficient magnitude. A real-valued matrix M, consisting of M columns and N rows is created:

$$M = \{ y_k(t_i) \}$$

Each column of the matrix corresponds to the time series that would be observed if only a narrow range of coefficient magnitudes contributed to the observed signal. A 3-D plot of the matrix M, called an **ampligram**, may be constructed. An ampligram covering 0 - 100% of coefficient magnitudes is called here the **total** ampligram. A total ampligram for the time series of monthly sunspot numbers in Fig. 1 is shown in Fig. 2.

The summation of the matrix M over k should result in the original sample $y(t_i)$, if there was no energy leakage from outside the filter band (6). The ampligram demonstrates the amplitude and phase of components of the signal corresponding to different spectral densities. The ampligram is a useful method for presenting the physical properties of the signal. The vertical (colour) scale of the ampligram has been limited to ± 5 in order to enhance the structure of the data around zero crossings.
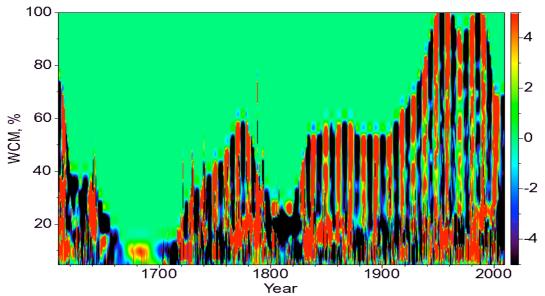
Fig. 2. The total ampligram of the time series of monthly values of the sunspot numbers in Fig. 1.

4. Time scale spectrum of an ampligram

The ampligram may be used for calculation of average wavelet spectra, one for each coefficient magnitude. It is equivalent to performing, once again, the forward wavelet transform on the filtered, inverse transformed data, which constitute the milligram. The transformation is applied to each row of the milligram matrix. The procedure generates a 3-D graph showing the time scale of the signal on the x-axis, the wavelet coefficient magnitude of the original signal (in percent of its max value) on the y-axis and the wavelet coefficient magnitude (corresponding to the power spectral density) of the decomposed component as the colour scale. A graph of that kind will show the average properties of the different modes, if such exist, during the entire sample period. As an example the time scale spectrum of the time series in Fig. 1 is shown in Fig. 3. Only scales shorter than 5.5 years are displayed.

It may be seen that, on average, for the whole period and magnitudes above 15% of the maximum, the spectrum is dominated by the 11-year solar cycle component.
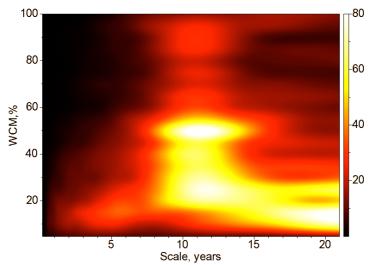

Fig. 3. The time scale spectrum (scales < 20 years) for the time series of Fig. 1.

5. Data analysis

The analysis of the sunspot number time series is performed using the Multiple Indicator Model (MIM) technique and Neural Network (NN) modelling. The methods have been described earlier (Liszka, 2003). The purpose of the MIM technique is to convert a univariate time series into a multivariate time series. This new multivariate time series consists of series of indicators describing the original time series. A suitable analysis window must be selected and properties of the original time series in the window are computed. The window is moved with a selected step length: in the present case, one month. In the present study a 32-point window has been selected. The 13 indicators used here are:

- Average
- Standard deviation
- Skewness
- Curtosis
- Median
- 8 spectral points of a scalogram (wavelet spectrum) in the time scale range 0.167-0.667 year

A working hypothesis is made, that there is precursor-information in the solar cycle preceding the beginning of a Grand Minimum. The selection of the window is a trade-off between the selection of the frequency interval carrying the precursor information and the highest possible time resolution.

During the investigated time series there are two Grand Minima: Maunder (1645-1715) and Dalton (1780-1839). Randomly selected 60% of the indicator matrix during the years 1610-1880 was used as a training matrix for a neural network model. A fourteenth column is added to the training matrix of indicators: ones during solar cycles preceding Grand Minima and zeroes during all remaining periods. The neural network model is based on a back-propagation NN with 13 inputs (indicators), 30 processing elements (PE) in the hidden layer and one single output (0/1). The recall data consisted of data during 1610-1880 not belonging to the training sample, and of all data between 1880 and February 2009.

6. Results of analysis

The result of recall with the entire recall data is shown in Fig. 4. An output of 1 indicates the presence of precursor information in the data, while 0 means that a Grand Minimum cannot be expected within the next solar cycle. An output of 0.5 indicates an inconclusive result.
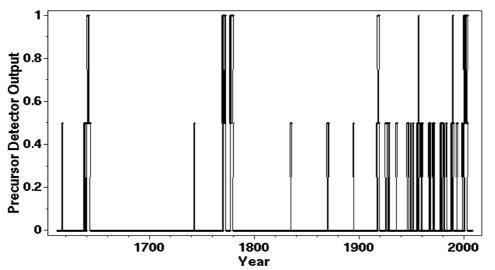

Fig. 4. The result of recall for the entire time interval 1610-2008.

It may be interesting to look more closely at how the model deals with recall data for the Maunder and Dalton Minima, see Figs. 5 and 6. The precursor detector outputs are plotted together with the original time series and the ampligram of the time series of monthly averages of sunspot numbers.
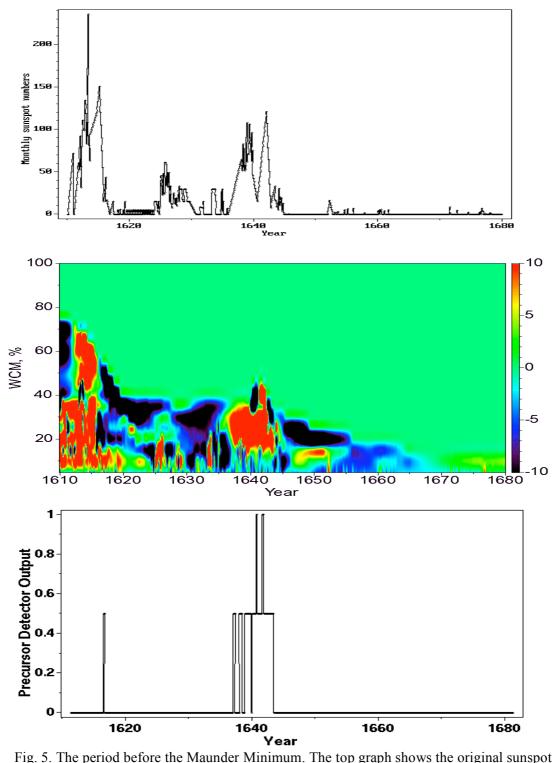

Fig. 5. The period before the Maunder Minimum. The top graph shows the original sunspot number time series and the middle graph shows the corresponding part of the total ampligram of Fig. 2. The bottom graph displays the output of the precursor detector.
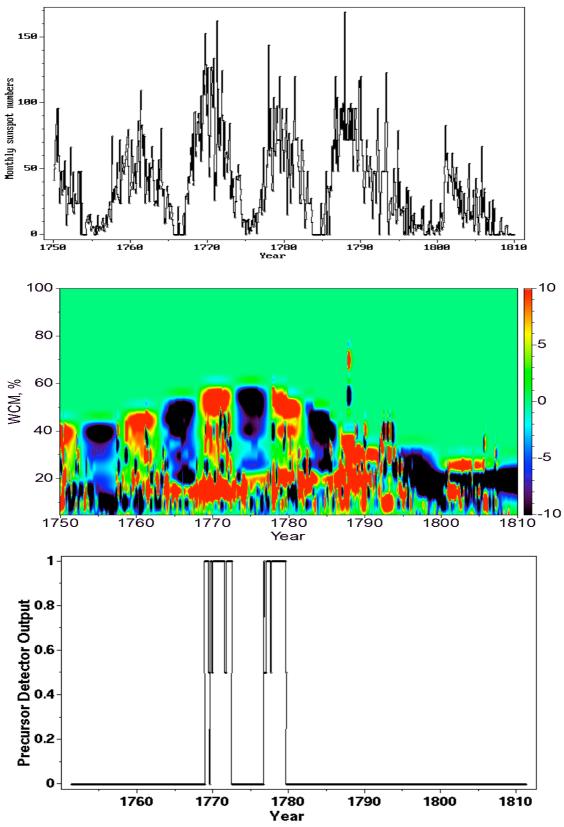
Fig. 6. The period before the Dalton Minimum. The top graph shows the original sunspot number time series and the middle graph shows the corresponding part of the total ampligram of Fig. 2. The bottom graph displays the output of the precursor detector.

An indication of the precursor information before the Maunder Minimum (Fig. 5) is not very conclusive, probably due to the poor quality of solar observations during the seventeenth century. The output for the Dalton Minimum is more distinct (Fig. 6). However it is not clear which structures of the wavelet spectrum may be responsible for the precursor information. A comparison with an Rg plot (group sunspot numbers) for the same period (top graph of Fig. 6) shows that the precursor information is most likely located around peaks of solar cycles.
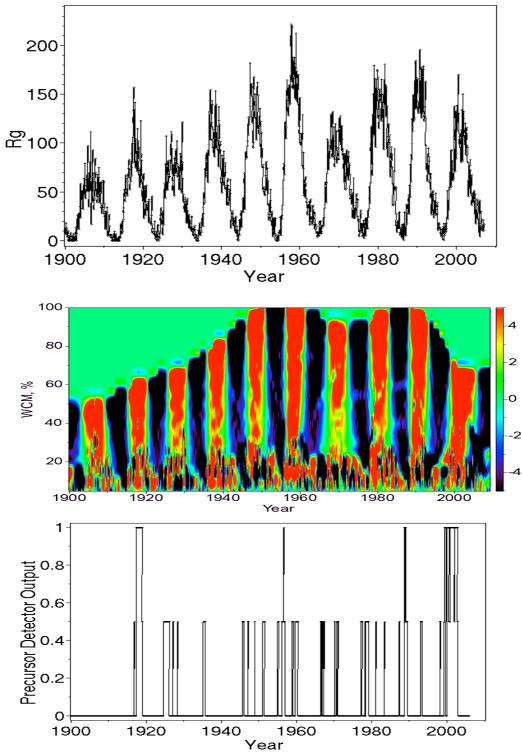

Fig. 7. The period 1900-2009. The top graph shows the original sunspot number time series and the middle graph shows its ampligram. The bottom graph displays the output of the precursor detector.

The purpose of the present study is to look closer at the period after 1900. The enlarged part of Fig. 1. for the years 1900-2007 is shown in Fig. 5 and the corresponding Rg plot in Fig. 6. There is a brief indication of the precursor information shortly before 1920, but a Grand Minimum apparently did not occur after it. A much clearer indication has occurred during recent years. The enlarged part of Fig. 7. for the years 1975-2008 is shown in Fig. 8.
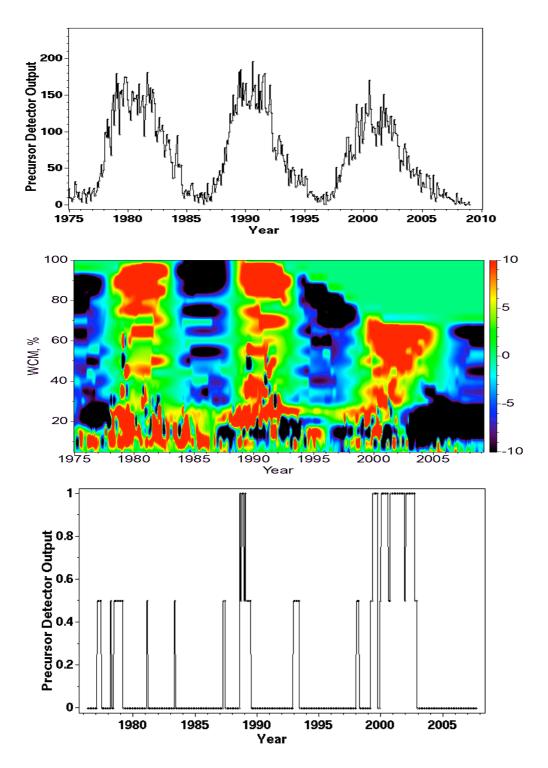

Fig. 8. The period between 1975 and Februay 2009. The top graph shows the original sunspot number time series and the middle graph shows the corresponding part of the total ampligram of Fig. 2. The bottom graph displays the output of the precursor detector.

Conclusions

The precursor information detected during years 2000-2003 is very clear. If the situation before the Dalton Minimum is repeated, it may be expected that the precursor information will repeat around the next solar maximum and that the next Grand Minimum will start approximately ten years from now. It is, of course, not possible to predict the severity of the approaching minimum.

Interesting conclusions may be drawn from the time scale spectra computed for different time intervals of the investigated periods. The resulting spectra for time scales < 5.5 years are shown in Fig. 9. The first time interval covers the years 1750-1810, just before the Dalton Minimum. The second time interval covers the years of stable solar activity between 1840 and 1890. The last one corresponds to recent years after 1975.
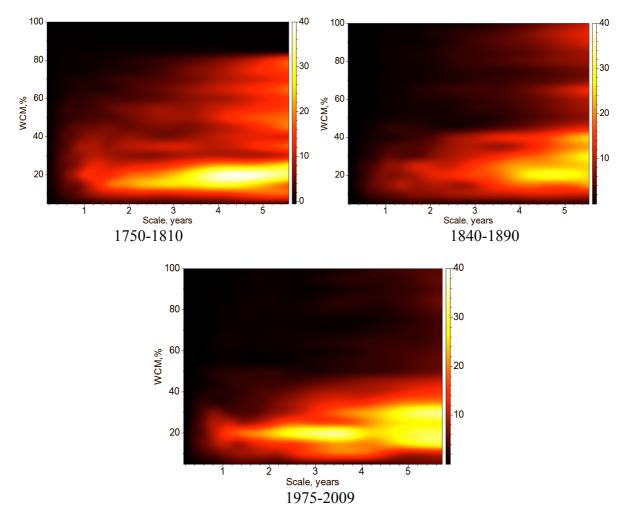

Fig. 9. Time scale spectra for scales < 5.5 years and periods (from the top): 1750-1810, 1840-1890 and for the years after 1975.

The present results indicate that the precursor information may be contained in semi-regular, short-periodical variations of solar activity.

References

Chui, C.K., *An Introduction to Wavelets*, Academic Press, Boston, 1992.

Chui, C.K., L. Montefusco and L. Puccio (eds.), *Wavelets: Theory, Algorithms and Applications*, Academic Press, Boston, 1994.

Farge, M., Wavelet transforms and their applications to turbulence, *Ann. Rev. Fluid Mech.*, 24, 395-457, 1992.

Farge, M., and Th. Philipovitch, Coherent structure analysis and extraction using wavelets, in *Progress in Wavelet Analysis and Applications*, eds. Y. Meyer, S. Roques, Editions Frontieres, Gif-sur-Yvette, pp. 477-482, 1993.

Lagoutte, D., J.C. Cerisier, J. L. Plagnaud, J. P. Villain and B. Forget, High-latitude ionospheric electrostatic turbulence studied by means of the wavelet transform, *Journal of Atmospheric and Terrestrial Physics* , 54, 1283-1293, 1992.

Liszka, L., *Cognitive Information Processing in Space Physics and Astrophysics*, Pachart Publishing House, Tucson, 2003.

Liszka, L., and M. Holmström, Extraction of a deterministic component from ROSAT X-ray data using a wavelet transform and the principal component analysis, *Astron. Astrophys. Suppl.* Ser 140, 125-134, 1999.

Wernik, A.W., and M. Grzesiak, Analysis of ionospheric plasma turbulence with the wavelet transform, in *Proc. Int. Symp. "Plasma 97", Jarnoltowek, June, 1997*, vol. 1, Space Research Center, Polish Academy of Sciences, pp. 391-394, 1997.